# Development of an Implantable Light Emitting Diode Device for the Photoconversion and Photoactivation of KikGR33 and Ai32 Mouse Models

[a] Hanna Rainiero*, [a] Jacky Tian*, [a] Ruochen Wang* , [a] Lisa Xiong*


[a] Department of Biomedical Engineering, University of Wisconsin-Madison, Engineering Centers Building, 1550 Engineering Drive, Madison, WI 53706


*Denotes co-first author*

**Corresponding Authors**

Hanna Rainiero and Lisa Xiong

Biomedical Engineering

Department of Biomedical Engineering, University of Wisconsin-Madison,

Engineering Centers Building, 1550 Engineering Drive, Madison, WI 53706

hrainiero@wisc.edu

pxiong55@wisc.edu

**Abstract**

There are increased research efforts to understand how the immune system responds to tuberculosis (TB), a serious infectious disease with an increasing presence of antibiotic resistance. Two mouse models, KikGR33 and Ai32, are used to investigate immune cell trafficking as an alternative therapeutic target using photoconversion (405 nm light) and photoactivation (450-490 nm light). The previous method for photoconversion/photoactivation involves a fiber optic cable with a needle attachment which lacks surface area exposure necessary for efficient photoconversion or photoactivation. As a proposed new method, PDMS-coated light emitting diodes (LEDs) assembled on a printed circuit board (PCB) were used and tested to be ultimately implanted into a mouse model for light delivery. Wavelength and intensity analysis, voltage vs. intensity analysis, brightness vs. intensity analysis, temperature analysis, and light scatter analysis using a gelatin brain mimic model were conducted to analyze LED behavior. The testing results showed that the LEDs can reliably emit light with appropriate wavelength and intensity. The biocompatible material PDMS coating the device would affect the light intensity without significantly changing the wavelength.Testings *in vitro* showed that the LEDs successfully photoconverted KikGR mouse cells and were found to be within the photoactivation range of the Ai32 mouse cells and the LEDs did not damage the cells as previously done with the fiber optic cable. In summary, the LED-PCB assembly is a safe and effective alternative to photoconvert and photoactivate immune cells which will aid the investigation of novel therapeutics for tuberculosis.

# 1. Introduction

## 1.1. TB current disease state and infection rates

Tuberculosis (TB) is a serious infectious disease that is among the top 10 causes of death globally, and is the leading cause of death from a single infectious agent [1]. Drug-resistant TB is a public health crisis with over half a million individuals developing TB with resistance to rifampicin, the most effective first line drug, and of those resistant, 82% had multiple drug resistant TB [1]. This clearly indicates a need for novel therapeutics to treat TB. A pathological hallmark of TB is granulomas, immune cell clustering around sites of infection, which is a potential target for therapy. Continuous cell replacement has been demonstrated as a mechanism of immune trafficking to maintain the granuloma microenvironment surrounding TB, however further research is needed in this area [2][3].

## 1.2. KikGR33 and Ai32 mouse models

They currently utilize two mouse models that express ion channels sensitive to light in their research: a KikGR33 mouse model which expresses green-red photoconvertible fluorescent protein at 405 nm and an Ai32 mouse model which expresses channelrhodopsins to allow photoactivation with exposed to 450 to 490 nm light (Fig. 1) [4]. Using a fiber optic cable, they illuminated small areas of affected tissue to photoconvert or photoactivate the cells. In KikGR mice, the lungs could then be excised up to seven days after photoconversion and examined to see the ratio of red immune cells that were photoconverted at the site to the green immune cells that were trafficked into the granuloma from unexposed tissue (Fig. 2) [2]. In Ai32 mice, calcium uptake by the cells can be observed to identify photoactivation.
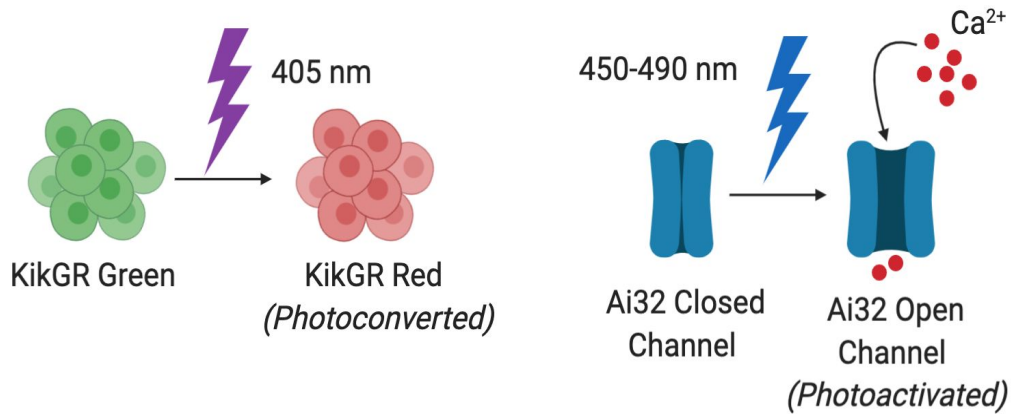
*Figure 1.* *The Sandor Lab uses two mouse models: KikGR which has photoconvertible cells when exposed to 405 nm wavelength and Ai32 which has photoactivatable cells that undergo calcium influx by channelrhodopsins after exposure to 450-490 nm light (Biorender).*
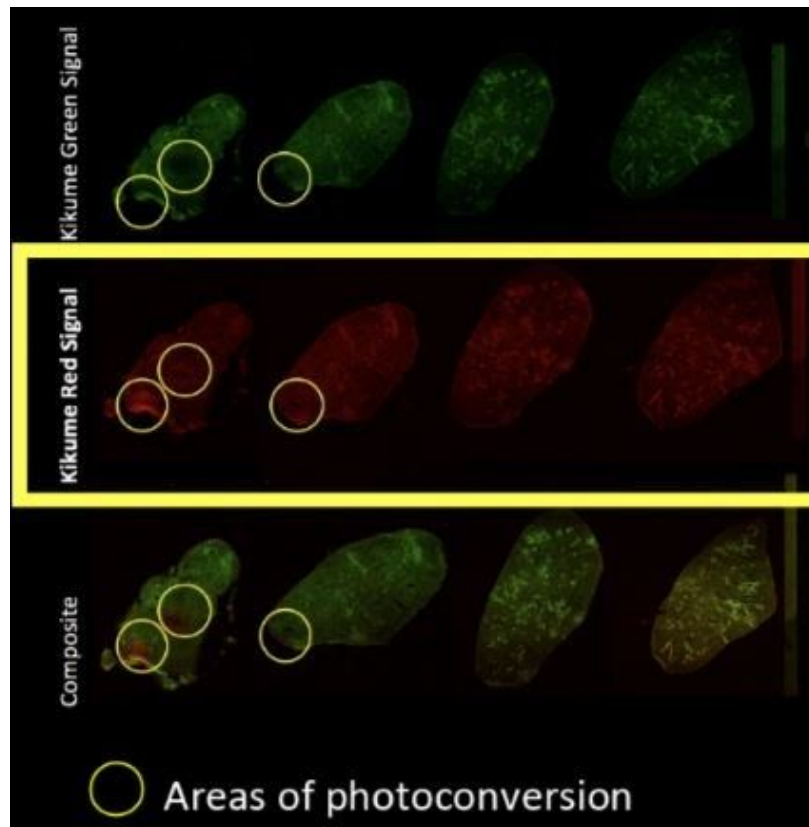


*Figure 2:* *Photoconversion by fiber optic cable is limited. Pictured above is fluorescent signalling from the lungs of KikGR33 mice infected with TB that had sites photoconverted by the fiber optic cable [2]. Note the small, inefficient area photoconverted (yellow circles) while the rest of the lung remains green. (Image courtesy of Dr. Matyas Sandor)*

## 1.3. Significance of LED

Fiber optic cables are inefficient in photoconversion/photoactivation. An LED implantable device was designed, fabricated, and tested for its photoconversion and photoactivation efficiency with KikGR33 and Ai32 mouse cells. Our device will mitigate the disadvantages of other current methods by being biocompatible, effective at photoconverting a larger area, and cheap to manufacture. Furthermore, our device will have implications for other research areas that utilize optogenetics. The implantable device includes LEDs as a light source for photoconversion or photoactivation, design of the LED circuit, and a safe, biocompatible coating for our final product.

## 1.4. Design specifications

A light strength of 95 mw/cm$^2$ light source has been cited as effective for photoconverting tissues [5][6]. Dr. Matyas has specified that an area of approximately 1 cm$^2$ is needed to illuminate the mouse lung. The wavelength necessary for photoconversion of KikGR33 fluorescent protein used in the client's mouse model is 405 nm [4]. Another mouse model used is the Ai32 mouse that needs a 450 - 490 nm wavelength and 400 mW/cm$^2$ light strength to activate channelrhodopsins. Our client has requested that we develop a light source specific to the Ai32 mouse into a device as well. The light should limit photodamage and phototoxicity to the tissue. The implant should be biocompatible and must not trigger an immune response in the mouse. The design specifications are further summarized with a table for clarification (Table 1).

**Table 1.** *Summary of the design specifications for different functionalities.*

|  | **Photoconversion** | **Photoactivation** |
|---|---|---|
| **Wavelength** | 405 nm | 450 - 490 nm |
| **Intensity** | 95 mW/cm^2 | 400 mW/cm^2 |
| **Size** | 1 cm^2 | 1 cm^2 |

| Heat Output | < 2°C locally < 1°C systemically | < 2°C locally < 1°C systemically |
|---|---|---|

The LEDs themselves must have the appropriate wavelength emission of 405 nm for successful photoconversion and 450-490 nm for photoactivation. The electronics must not cause excessive heat within the mouse. The Association for the Advancement of Medical Instrumentation (AAMI) recommended that an implant should not increase the systemic body temperature by more than 1°C and the local area should not increase by above 2°C [7]. Additionally, tissue coagulation will occur between 50°C and 60°C, so the implant must remain well below that temperature threshold [8].

Considerations for our biomaterial coating include optical clarity, biocompatibility, and electronic inertness. Common biomaterials used to encapsulate medical devices that are optically clear include silicones and parylenes. Parylene C is the gold standard for encapsulating electronic devices due to its optical clarity, high dielectric constant, and low permeability to water and chemicals [9][10][11]. Medical grade silicones can also be used for encapsulating devices, however their biocompatibility is less ideal than Parylene C [12].

There are devices available on the market for the photoconversion and photoactivation of KiKGR33 and Ai32 mouse cells. Devices used for photoconversion in previous scientific studies are the USHIO SP500 and SP250 spot UV curing equipment and Leica Microsystems fluorescence stereo microscopes (Fig. 3A) [5][6][13]. Prabhakar et. al [14] used a Fibertec II Fiber Coupled Diode Laser Module (Blue Sky Research) to photoactivate Ai32 mouse cells whereas Madisen et. al [15] used a 200-μm optical fiber coupled to a 593-nm yellow laser (Fig. 3B). Although these devices may already be on the market, none of them utilize LEDs as a source of light, these current devices can be expensive and are not as convenient to operate as LEDs.
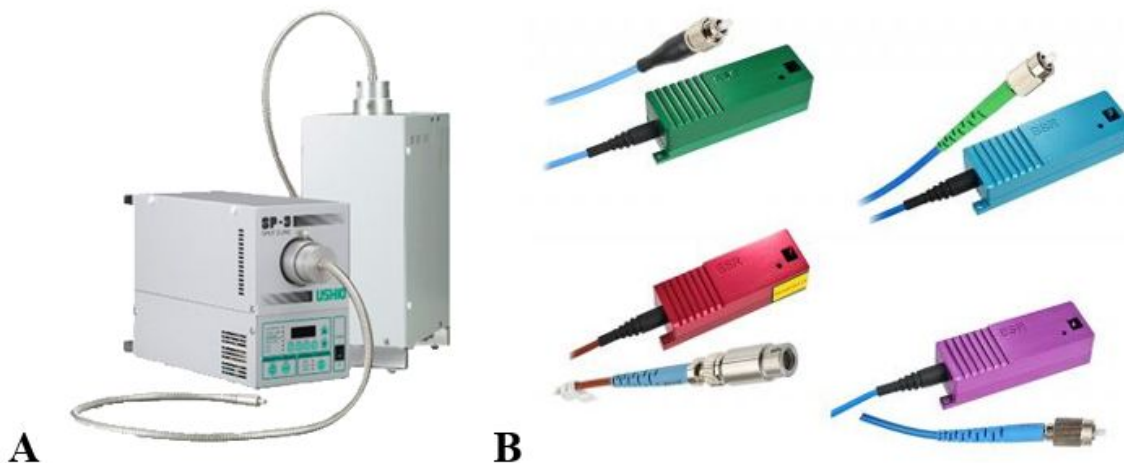
**Figure 3: A,** *The USHIO Spot-Cure Series, Spot UV Curing Equipment uses a low attenuation UV lamp [16].* **B,** *Blue Sky Research's FiberTec II™ Series uses fiber-coupled lasers that incorporate modulation and feedback functions [17].*

## 2. Materials and Methods

### 2.1. Electronics

405 and 465nm LEDs (Vishay Semiconductors, Malvern PA, USA and Changzhen Village, Guangming New District, Shenzhen, China) with solder mask defined pads (SMD) were purchased for the photoconversion and photoactivation of the KikGR33 and Ai32 mouse models respectively. The dimension of the 405nm LEDs is 3.2 mm x 2.8 mm x 1.9 mm and has a fixed wavelength and requires 20mA or 3.2V to operate [18]. The dimension of the 465nm 5050 RGB LEDs is 5mm x 5mm. It has an integrated driver chip and requires approximately 18mA constant current drive to operate [19]. The integrated driver chip allows additional functionalities to control the brightness, wavelength, and pulse width modulation using a NodeMCU ESP8266. The NodeMCU ESP8266 is compatible with the clockspeed used to control the 465nm LEDs.

### 2.2. Printed circuit board fabrication

A printed circuit board (PCB) was designed using *Altium Designer* (San Diego, CA), a commercial and electronic design automation software package for designing PCBs, to provide

power and control to the LEDs. Two 405nm LEDs are connected in parallel to 3.3V (VCC) and ground (Fig. 4) to the microcontroller (MCU).
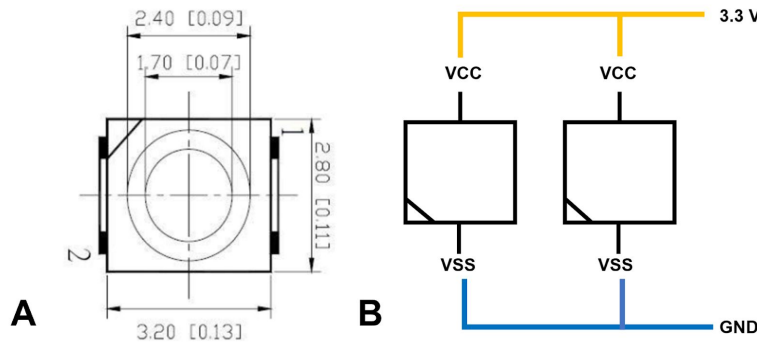


*Figure 4: A, The 405 nm LED is a 2 pin device, powered with 0-3.3 V (pin 1) and connected to ground (pin 2, units in mm) [18]. B, LTSpice was used to create the circuit schematic. The PWR symbol represents a power supply of +3.3 V which is input into pin 1 of the LED represented by the triangle-vertical line symbol. It is then connected to the ground.*

Four 465nm LEDs are connected in parallel to provide the same amount of voltage to all LEDs (Fig.5). There are 4 pins on the 465 nm LEDs: pin 1 is for grounding the LED, pin 2 is used for control input signal data, pin 3 is for power supply, and pin 4 is for control output data. For the specification of the LED manufacturer, pin 4 of the previous LED must connect to pin 2 of the next LED for simultaneous control. The PCB designed fulfills the necessary connection requirement.
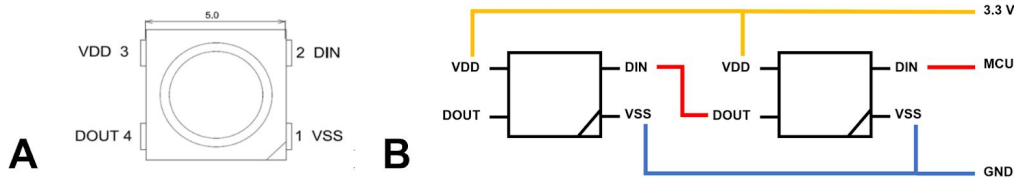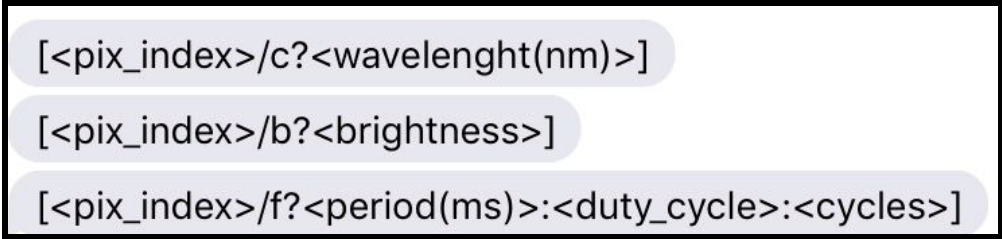


*Figure 5. A, The 465 nm LED is a 4 pin device. Pin 1 (VSS) is the ground pin, pin 2 (DIN) is the digital input pin that communicates with the microcontroller, pin 3 (VDD) is the power pin where +3.3 V is input, and pin 4 (DOUT) is the digital output pin where the LED can send the signal it receives from the microcontroller to other LEDs [19]. B, The 465 nm LEDs were powered in parallel (+3.3 V) through the Vcc pin of the microcontroller (represented by the Input2 symbol), connected to ground through the GND pin of the microcontroller, and the LED designator 1 communicated to the microcontroller (pin 2 LED to pin 1 of Input2).*

## 2.3. Bantam-milled PCB Prototypes

A desktop PCB milling machine (Bantam Tools, Peeksill, NY) was used to mill the PCBs for the LED connections. The PCBs were not manufactured professionally so that prototyping, testing, and debugging of code and electrical connections could be possible early in the fabrication and testing stage. The Altium files were output into compatible Bantam files and loaded into the milling machine for fabrication. A total of eight 405 nm PCBs and four 465 nm PCBs were produced.

## 2.4. Arduino code

Code was developed on Arduino to allow users of the 465 nm LED to change the wavelength, brightness, and pulse width modulation using the serial monitor (Fig. 7). Within the code there is a wavelength to RGB conversion; however, the Neopixel only can simulate the appearance of a color with three different wavelengths: red, green, and blue. As a result, the wavelength used must rely solely on the blue pixel of the Neopixel and the code is currently being used to control the brightness and pulse width modulation of the blue pixel within the Neopixel. An advantage of incorporating pulse width modulation is that the LED will emit light at frequencies close to which the channelrhodopsins fire so that the channels are not exposed during their refractory period before they can fire again. The pulse width modulation will also conserve more energy since it is not powered constantly and will reduce phototoxicity and heat production.



```
[<pix_index>/c?<wavelenght(nm)>]
[<pix_index>/b?<brightness>]
[<pix_index>/f?<period(ms)>:<duty_cycle>:<cycles>]
```

**Figure 6.** *The format of the command input for Arduino.*

## 2.5. Testing

### 2.5.1. Wavelength and intensity

For wavelength and temperature testing, an Ocean Optics Spectrophotometer (USB2000+) was used to collect wavelength and intensity data from the LEDs. In order to minimize saturation of the spectrophotometer, the LEDs were kept at a distance of 35.81mm from the spectrophotometer (Fig. 8). A similar testing setup was done for the 405nm LEDs. However, because of the non-programmable LED intensity, the sensor was placed at a much further distance of 659.16mm. Ten wavelength and intensity data was collected to identify the consistency of the LEDs with standard error calculations and to identify the mean wavelength range and mean peak within the required intensity range for each of the LEDs. Measurements of PDMS coated and uncoated LEDs were also measured to compare the effect of PDMS on the LED wavelength and light intensity.
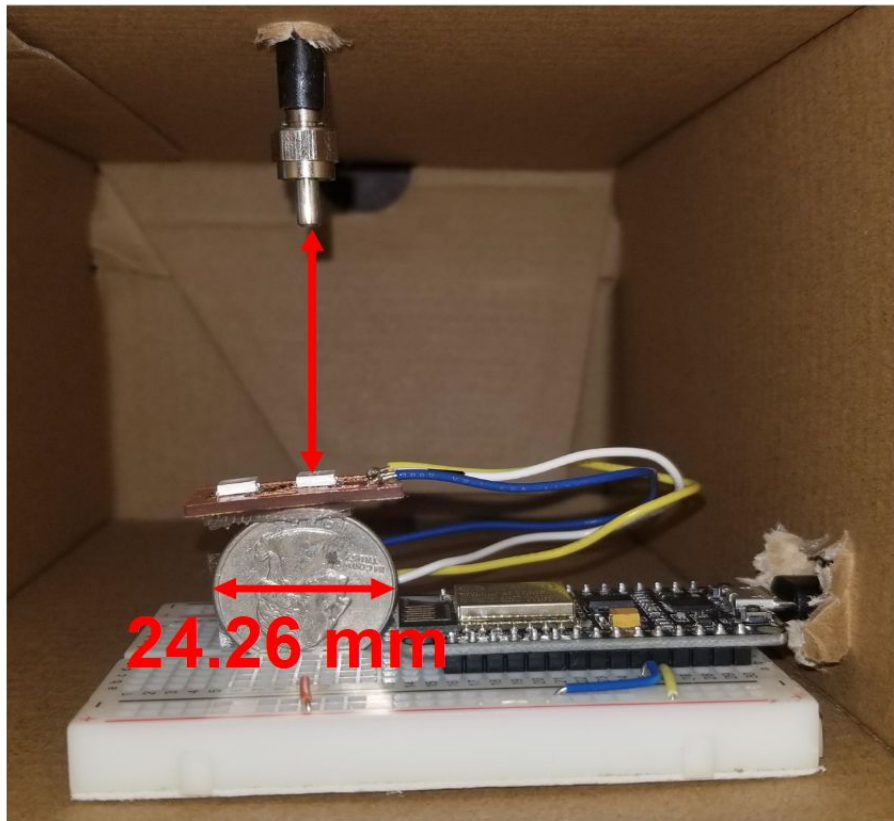


*Figure 7*: The testing schema of light intensity using the Ocean Optics Spectrophotometer USB2000+. Quarter for size reference.

## 2.5.2. 405nm Voltage vs. Intensity

When the 405nm LEDs are connected to a 3.3V power source, the LEDs will emit the maximum light intensity at a 405nm wavelength. To develop a user-friendly method of controlling light intensity, a three pin linear rotary potentiometer was connected between power and the LED to limit the input voltage (Supplement 7.2). The potentiometer allowed for control of resistance and voltage supplied to the LED using a dial (Fig. 8).
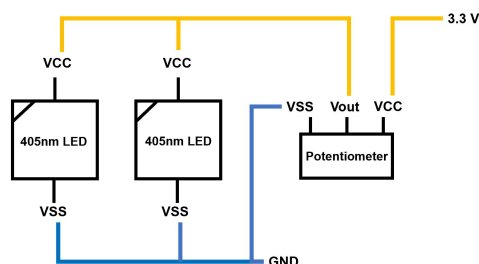


**Figure 8.** *The schematic shows the placement of the potentiometer in the 405nm connections. Vout outputs a voltage into VCC of the 405nm LEDs.*

The 405nm LEDs were set at a perpendicular distance of 659.16mm from the spectrophotometer sensor. A digital multimeter was used to measure the voltage between VSS and Vout at the maximum light emittance to the lowest visible light emittance. Intensity of the 405nm LEDs were measured at the following voltages: 2.84V, 2.88V, 2.93V, 2.97V, 3.03V, 3.06V, 3.08V, 3.10V, and 3.15V, where 3.15V was the maximum voltage measured when the dial was at its minimum resistance. Three measurements were taken at each voltage step. Intensity of the PDMS coated and non-coated LEDs against voltage were measured and analyzed with linear regression.

### 2.5.3.    465nm Program Brightness vs. Intensity

The programmed brightness of the 465nm LEDs can be used to control the intensity of the LED light. The testing setup of the 465nm LEDs is the same setup mentioned in section 2.4.1. Three intensity measurements were taken at five levels of arduino code brightness: 1, 2, 3, 4, and 5. Their corresponding real-time brightnesses are 0.39%, 0.78%, 1.18%, 1.57%, and 1.96%. Intensity of the PDMS coated and non-coated LEDs against program brightness were measured and analyzed with linear regression.

### 2.5.4. Temperature testing

Change in temperature of the LED *in vitro/in vivo* was simulated by measuring the change in temperature of phosphate-buffered saline (PBS) solution with the PDMS encapsulated PCB over a duration of two hours (Fig. 9).
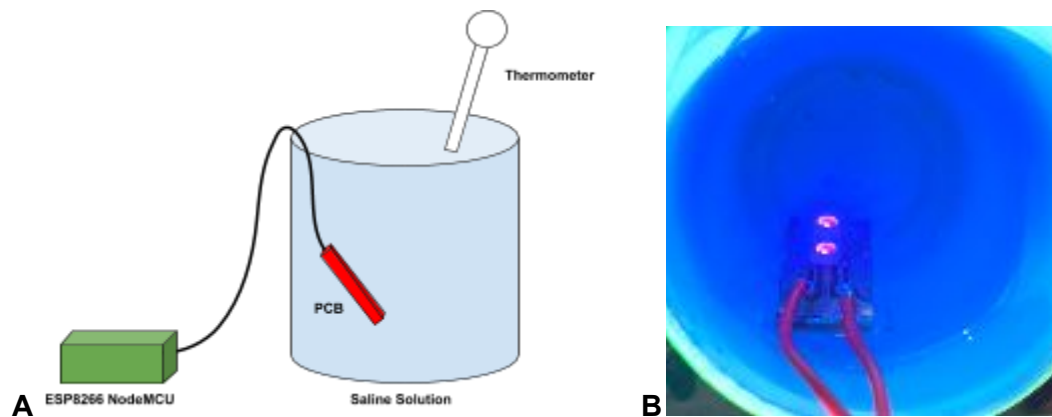


**Figure 9.** A, *The PDMS encapsulated PCB is placed in a saline solution and connected to the microcontroller. The starting temperature is 20°C (room temperature) and recorded every 10 minutes for two hours. B, 405 nm LED in tap water (preliminary testing).*

The saline solution temperature was sampled every 10 minutes and then analyzed using *VassarStats*. Regression statistics were performed to identify the relationship and variation of temperature of the LEDs over time and to assess if it stayed below the temperature threshold.

### 2.4.5 In vitro testing (KikGR mouse model)

A cell suspension of KikGR mouse lymph node cells were pelleted in a 1.7 mL clear, conical tube (Fig. 10A).The tube was placed on top of the 405 nm LED for 5 and 15 min with a 0 min exposure control (Fig. 10B). After exposure, the cells were resuspended, pipetted into a slide counter, and imaged under a confocal microscope. With no exposure to 405 nm wavelength light, the Kikume protein emits 517 wavelength light (green) under a fluorescent microscope when excited by a green laser (488 nm). With exposure of a 405 nm wavelength, the Kikume protein undergoes a conformational change and emits red (593 nm) when visualized under a fluorescent microscope after excitation with a red laser (594 nm). Cell viability was also assessed using Trypan blue following ~30 minutes after LED exposure.
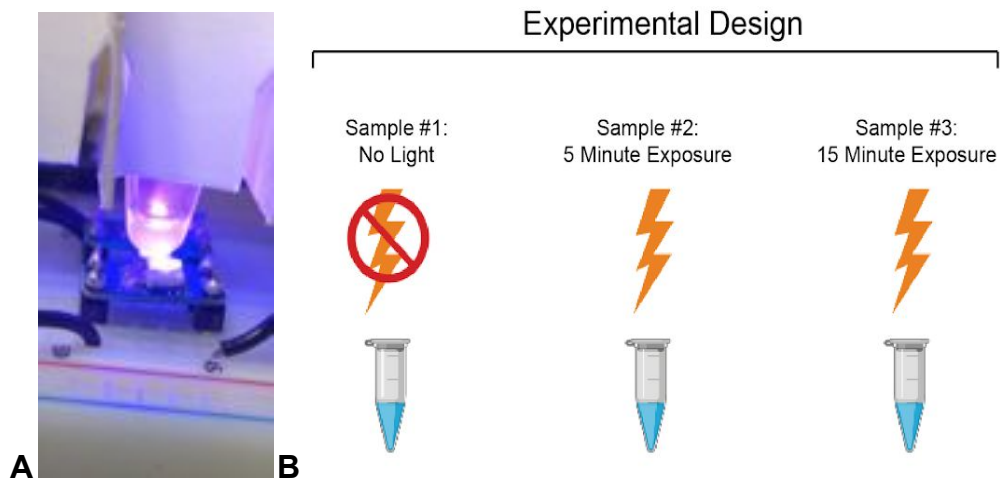
**Figure 10.** *In vitro testing of KikGR cells with 405 nm LED. A lymph node cell suspension of KikGR cells was pelleted in a 1.7 mL clear, conical tube and placed directly on the 405 nm LED (A) for 5 and 15 minutes with a 0 min exposure control (no exposure) (B).*
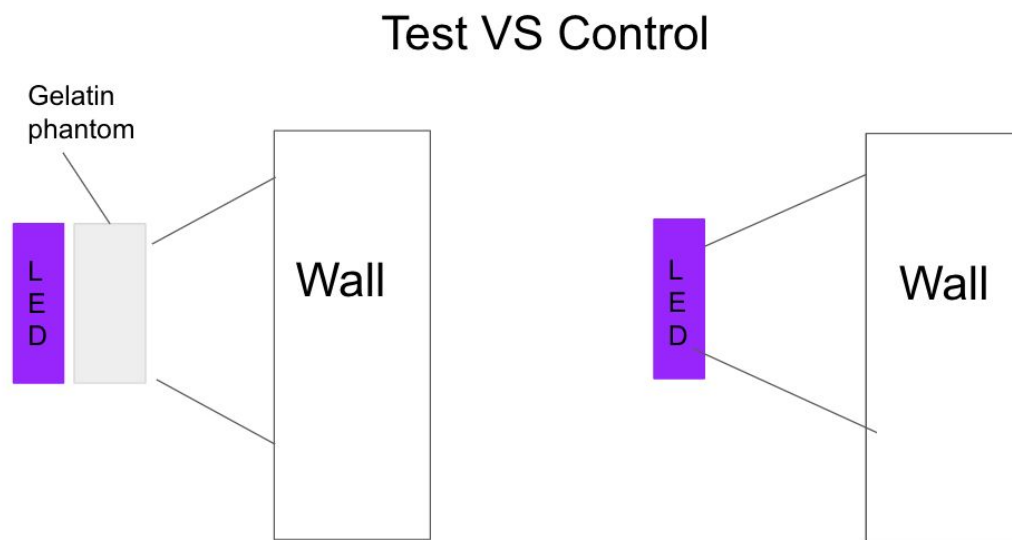
*2.6.    Gelatin Light Scattering Simulation*



**Figure 11**: *The light scattering experiment setup for 405nm LED. The photo of the wall is taken to the find the range of the light for comparing the light scattering*

The light scattering pattern in the brain was simulated by shining the 405nm LED through the brain tissue phantom made with gelatin to the wall in a dark room. The same 405nm

LED is shined with the same distance away from the wall as the control to compare the difference. The brain tissue phantom gelatin is made with 50% of the water replaced by milk, and it exhibits similar photoacoustic properties to that of the brain tissue [20]. The light scattering pattern on the wall was recorded by taking a photo with an iphone and the image is further processed with imageJ to measure the scattering of the light.

## 2.7. Statistical Analysis

The wavelength and intensity of PDMS coated and uncoated LEDs would be analyzed with a paired two sample t-test for means. The voltage vs. intensity and brightness vs. intensity data would be analyzed with a regression analysis. The goal of the voltage vs. intensity and brightness vs. intensity analysis is to understand the relationship and develop an equation to potentially program future prototypes to control light intensity.

## 3. Results

### 3.1. Device validation

#### 3.1.1. Bantam-milled PCB Prototypes

The PCBs produced by the Bantam mill are fully functional, showing that the PCB connections and schematics are feasible for this project. The PCBs prototypes produced are not intended for implantation as they are solely for testing purposes (Fig. 12).
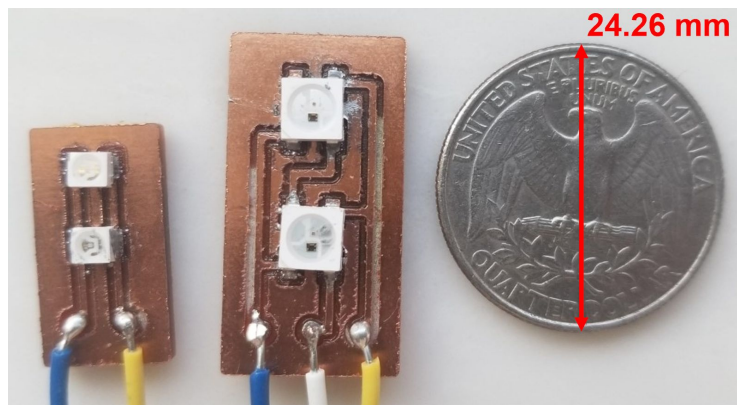


**Figure 12.** *The PCB on the left contains the 405 nm LEDs and the PCB on the right contains the 465 nm LEDs. Both are compared to the size of a quarter.*

#### 3.1.2. LEDs meet Wavelength and Intensity Requirements

For the Blue LEDs, the mean lower bound wavelength at 400 mW/cm$^2$ was 449.9 nm (SE=4.02x10$^{-14}$ nm) and the mean upper bound wavelength was 486.9 nm (SE = 0.1 nm). The peak wavelength and intensity was 465.2 nm (SE= 0 nm) and 520.73 mW/cm$^2$ (SE = 2.46 mW/cm$^2$) (Fig. 13). For the 405 nm LEDs, the mean lower bound wavelength at 95 mW/cm$^2$ was 392.2 nm (SE=0.1 nm) and the mean upper bound wavelength was 420.6 nm (SE = 6.96x10$^{-14}$ nm). The peak wavelength and intensity was 405.7 nm (SE= 0.1 nm) and 501.9 mW/cm$^2$ (SE = 1.75 mW/cm$^2$) (Fig. 13).
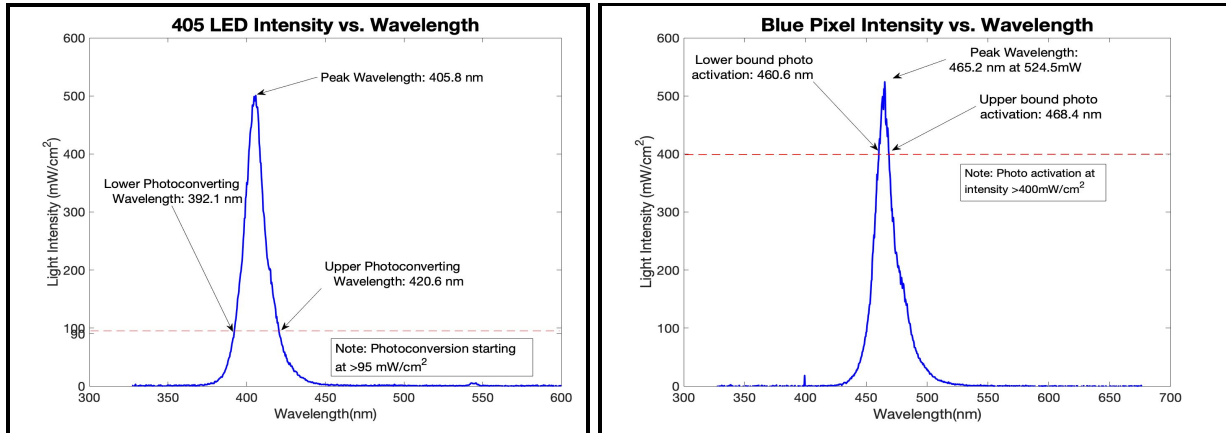


**Figure 13.** *Identifying photoconverting/activating wavelength range of LEDs. Device was tested in triplicates using Ocean Optics Spectrometer (USB2000+). The photoconvertible range of the 405 nm LED is on average from 392.2 nm and 420.6 nm with a peak wavelength at 405.8 nm and intensity of 501.9 mW/cm2. The blue LED photoactivating range is on average from 449.9 nm and 486.9 nm with a peak wavelength at 465.2 nm and intensity of 520.73 mW/cm2 (MATLAB).*

### 3.1.3.   PDMS Coating does not impact wavelength but does impact intensity of LED

The paired t-test analysis revealed that PDMS coating does not significantly impact the wavelength of an LED when compared to its uncoated counterpart (significance value of $p$=0.05) (Figure 14). The paired t-test analysis revealed that PDMS coating did significantly impact the intensity of an LED when compared to its uncoated counterpart ($p$=0.001 for 405nm and $p$=2.76E-12 for 465nm LEDs).
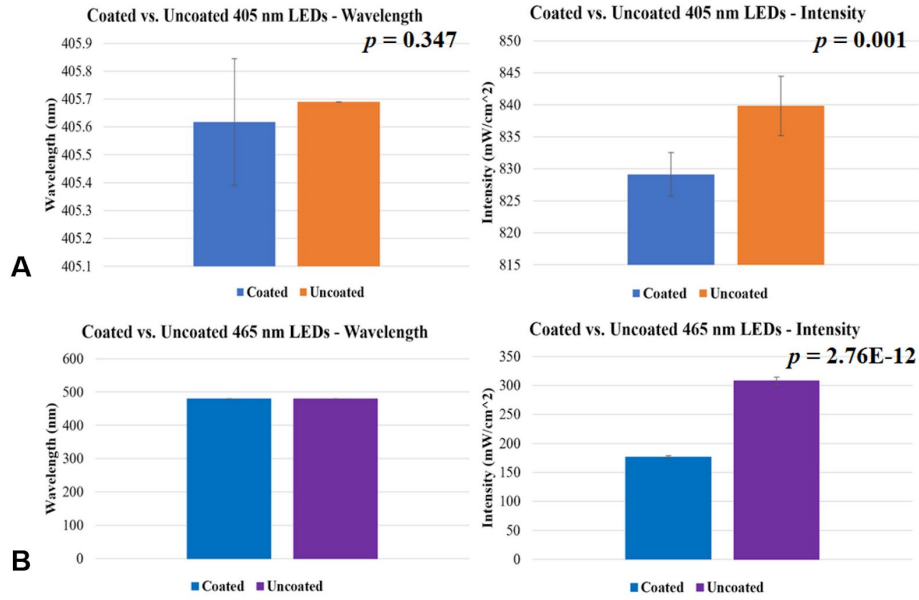
***Figure 14. A,*** *Average wavelength and intensity measurements for uncoated and coated 405nm LEDs were compared to each other. Using a significance value of p=0.05, there were no significant differences in the mean for the wavelength (p=0.347) but significant differences for the intensity (p=0.001).* ***B,*** *Average wavelength and intensity measurements for uncoated and coated 465nm LEDs were compared to each other. The mean was exactly the same for the 465nm wavelength measurement. Using a significance value of p=0.05 there was a significant difference in the mean for the intensity (p=2.76E-12).*

### 3.1.4.    405 nm LED Voltage vs. Intensity Relationship Validation

The voltage vs intensity was a nearly linear relationship ($R^2$ = 0.932) which will be able to be used in the future when optimizing photoconversion and minimizing phototoxicity for the LED as we can modulate the intensity of the LED through the voltage used to power them (Fig. 15). Consideration for decreased intensity with coated LED should be assessed. Variation in LED intensity seen ~3.1V may be attributed to confounding factors in test setup such as shifting of LED or background light.
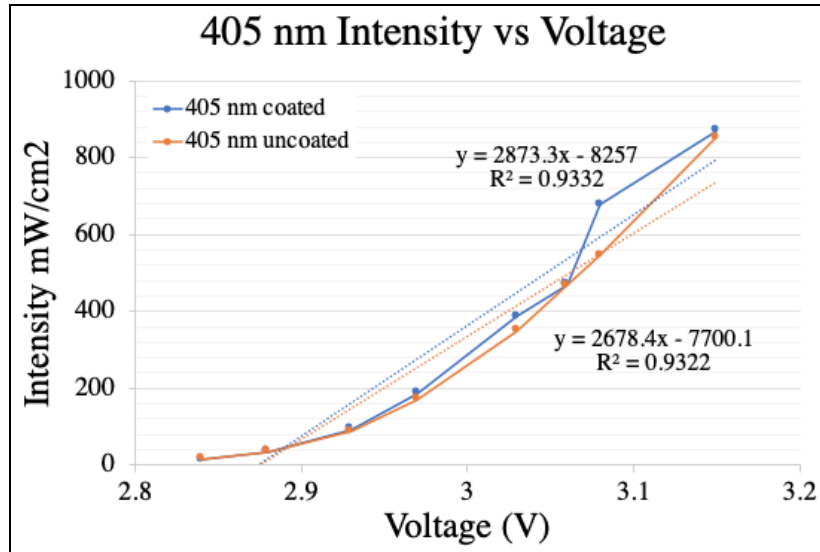
16

***Figure 15.*** *Intensity vs Voltage for 405 nm LED PCB. Both the uncoated and coated 405nm LEDs exhibited the same linear behavior when voltage was controlled to manipulate the intensity.*

*3.1.5.    465nm LED Program Brightness vs. Intensity Relationship Validation*

The brightness vs intensity was a nearly linear relationship ($R^2$ = 0.99) which will be able to be used in the future when optimizing photoconversion and minimizing phototoxicity for the LED as we can modulate the intensity of the LED through the brightness entered in the Arduino program (Fig. 16). Consideration for decreased intensity with coated LED should be assessed.
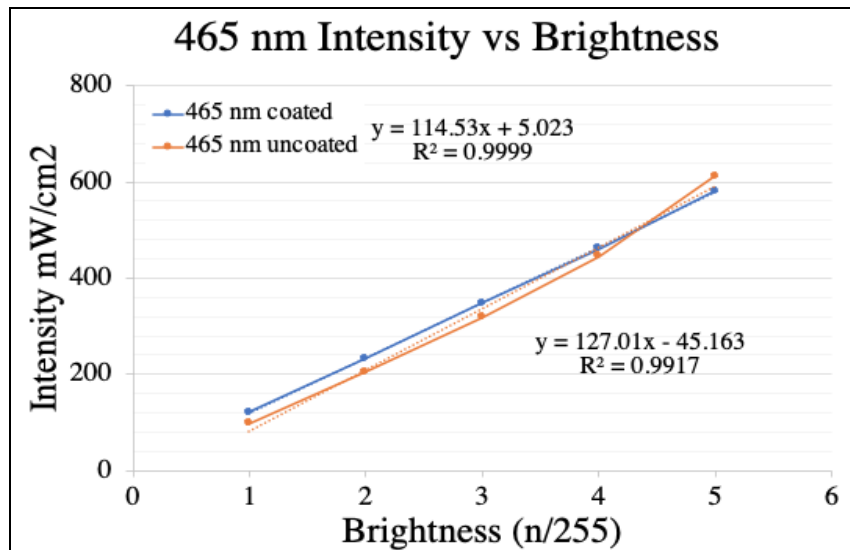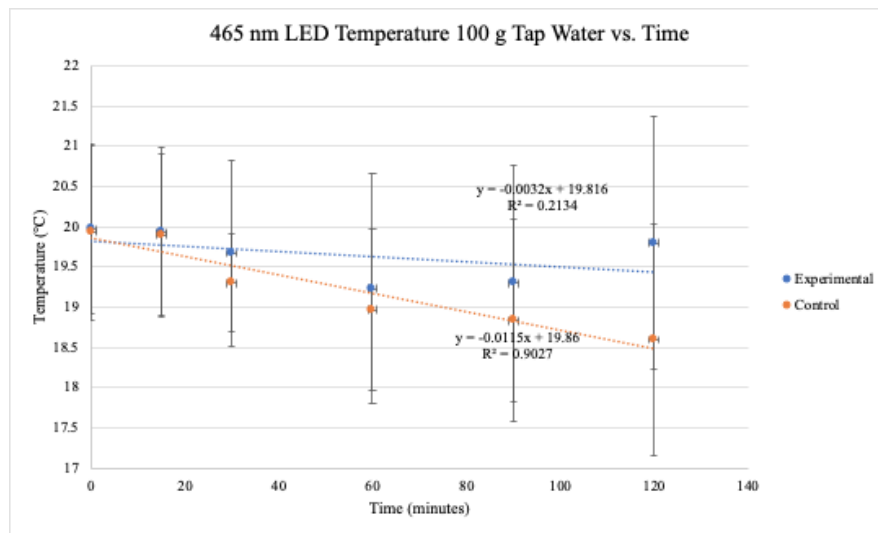


***Figure 16.*** *Intensity vs Brightness for the 465nm RGB LED. Both the coated and uncoated LED exhibited linear behavior when brightness was controlled to manipulate the intensity. Brightness is defined in the*
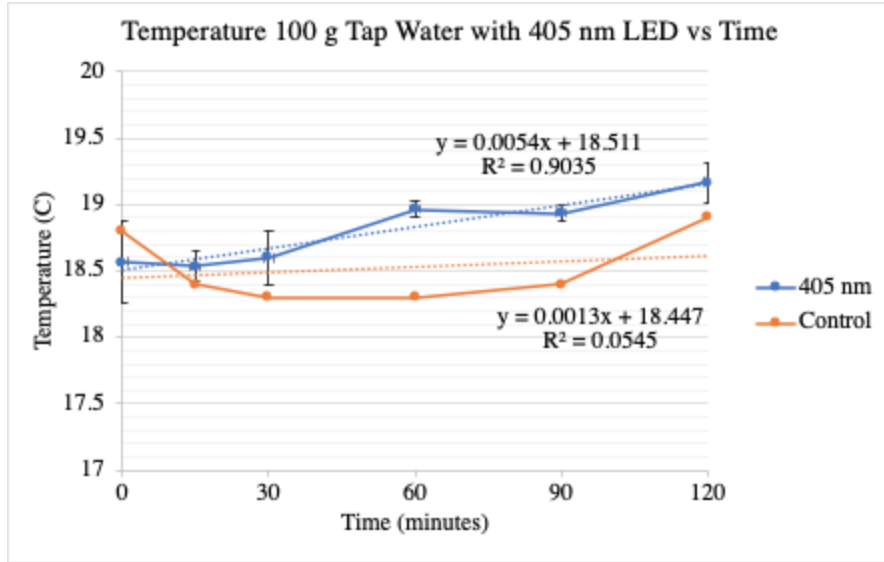
*code as a value between 0 and 255 because of the 256 RGB pixel LED. A max brightness of 5 was chosen as to not saturate the spectrophotometer.*
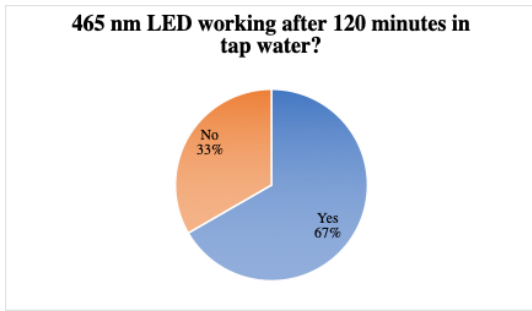
### 3.1.6.    Temperature and Durability Testing

Temperature of 100 g of tap water was monitored over the course of two hours with coated PCBs operating and submerged in the water. 465 nm LED water temperature was measured with a fish tank thermometer resulting in greater deviation of temperature readings; no significant increase or correlation was observed. The 405 nm LED water temperature was measured with an infrared laser thermometer allowing more precise readings. A slight increase in temperature was observed however the LED remained within the specifications recommended for implantation (Fig. 17). PCB was assessed for durability measure by observance of corrosion and/or stopping working. 33% of LEDs in both the 405 nm group and the 465 nm group developed corrosion (one in each group). The PCB in the 465 nm PCB group stopped working and had to be reprogrammed.

**465 nm LED Temperature 100 g Tap Water vs. Time**

$y = -0.0032x + 19.816$
$R^2 = 0.2134$

$y = -0.0115x + 19.86$
$R^2 = 0.9027$

A

## Temperature 100 g Tap Water with 405 nm LED vs Time

$$y = 0.0054x + 18.511$$
$$R^2 = 0.9035$$

$$y = 0.0013x + 18.447$$
$$R^2 = 0.0545$$

405 nm

Control

**B**

## 465 nm LED working after 120 minutes in tap water?

No 33%

Yes 67%

**C**

## Any presence of corrosion on 465 nm LED?

Yes 33%

No 67%

**D**

## 405 nm LED working after 120 minutes in tap water?

No 0%

Yes 100%

**E**

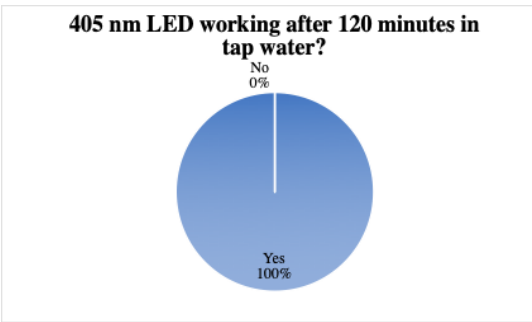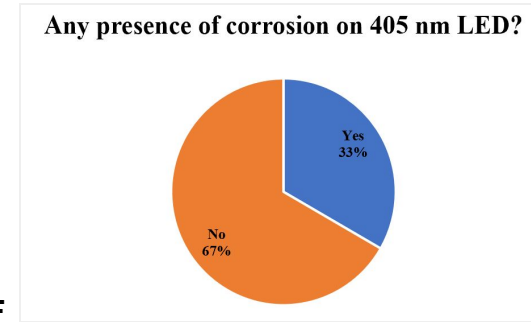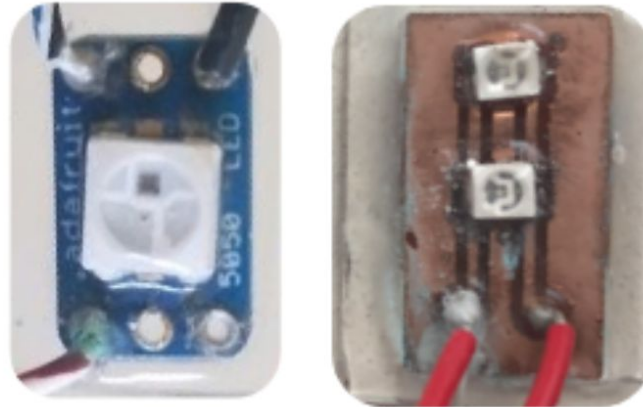## Any presence of corrosion on 405 nm LED?

Yes 33%

No 67%

**F**

19

**G**

*Figure 17. A-B,* Change in temperature of the water containing the coated 465 nm LED was not statistically significant from the control (p=0.086). Change in temperature of the water containing the coated 405 nm LED was statistically significant from the control (p=0.049), however, LED is still within design specifications. *C-F,* Pie charts depicting functionality and presence of corrosion after six hours of testing. *G,* Apparent corrosion despite PDMS coating occured in 33% of LEDs tested and caused one LED to stop working and reprogrammed with Arduino code.

### 3.2. LED more diffuse and wavelength shifted when shone through gelatin mimic

The projection of light passed through a gelatin brain phantom mimic showed diffusivity and a wavelength shift as a result of scattering through the phantom (Fig. 18).
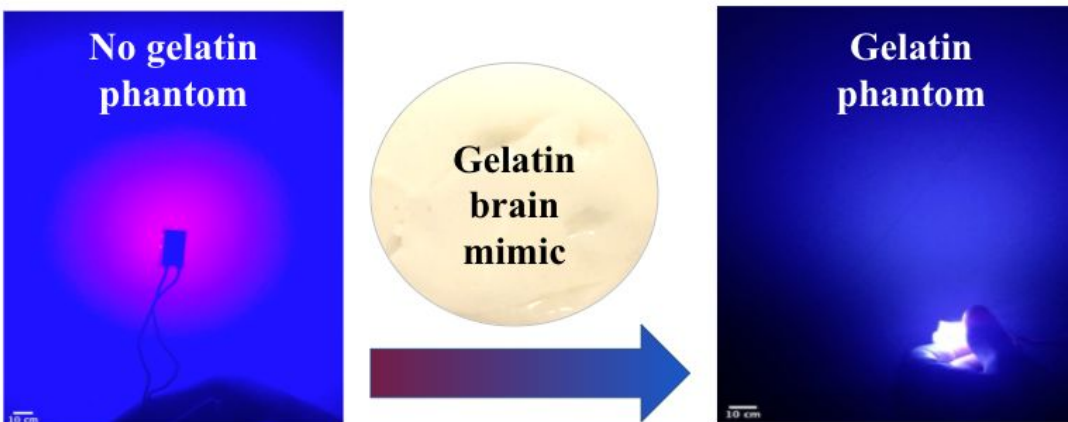


*Figure 18.* The 405nm shines through gelatin phantom, significant shift of the light wavelength, decrease in light intensity and the light covers more area than before is observed.

### 3.3. In vitro photoconversion observed in 5 minute and 15 minute exposure groups

Photoconversion was observed with the 5 and 15 min exposure photoconverting the cells from green to red (Fig. 19A). The mean intensity of the 0 min exposure was on average 18.84 AU for KikGR green and 7.10 AU for KikGR red (standard deviation (std) = 4.92, standard error of the mean (SEM)=0.492 and std = 0.37, SEM=0.037 respectively). The exposed cells at 5 and 15 minutes showed on average 7.2 AU and 6.3 AU for KikGR green (std=0.57, SEM=0.057 and std=0.623 and SEM=0.06 respectively) and 22.98 AU and 22.49 AU for KikGR red (std = 4.85, SEM=0.485 and std=2.79, SEM=0.279 respectively) (Fig. 19B). In a two-way ANOVA the 5 and 15 minute exposure groups were significantly different from the 0 min exposure control (p<0.0001). There was no statistically significant difference between the 5 minute and 15 minute exposure group. Cell viability assessed with trypan blue was shown to be unaffected between experimental groups shortly after exposure to the LEDs (Fig. 19C).
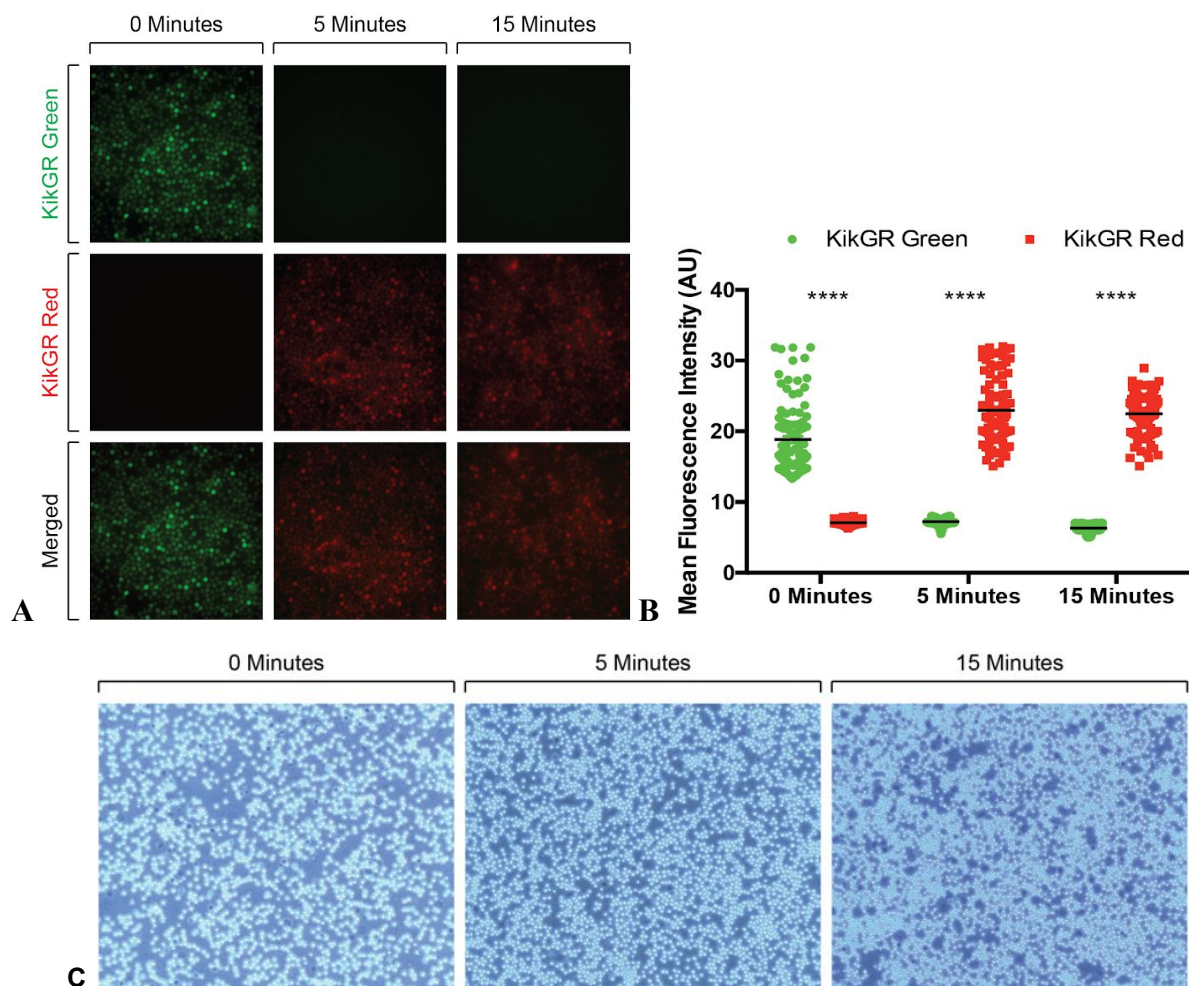
## 4.  Discussion

The PCB prototypes and the connections designed in Altium were successful and fully operational. Previously, the 465nm LED PCB board could not be tested due to the small size of the LED footprints that were printed from the PCB manufacturer. The LEDs were successfully encapsulated with a biocompatible coating, PDMS. When comparing PDMS coated and uncoated LEDs, we found that coating only significantly impacted the intensity. In addition, the heat output of the LEDs in a water test is safe for *in vivo* studies. The voltage vs. intensity and brightness vs. intensity analysis resulted in linear equations with high $R^2$ values. As a result, these equations can be used to calculate and obtain the desired intensity by manipulation of voltage or program brightness. The manipulations of intensity by controlling these variables can help prevent strong light intensities. Although PDMS is biocompatible, there was evidence of corrosion to our LEDs (Fig. 20).The light scattering is also significant and observable even though the LED light intensity fulfilled the client's requirements. However, the thickness of the gelatin phantom was 6mm and more testing could be conducted with various thickness of gelatin in the future to test for the thickness it could penetrate.
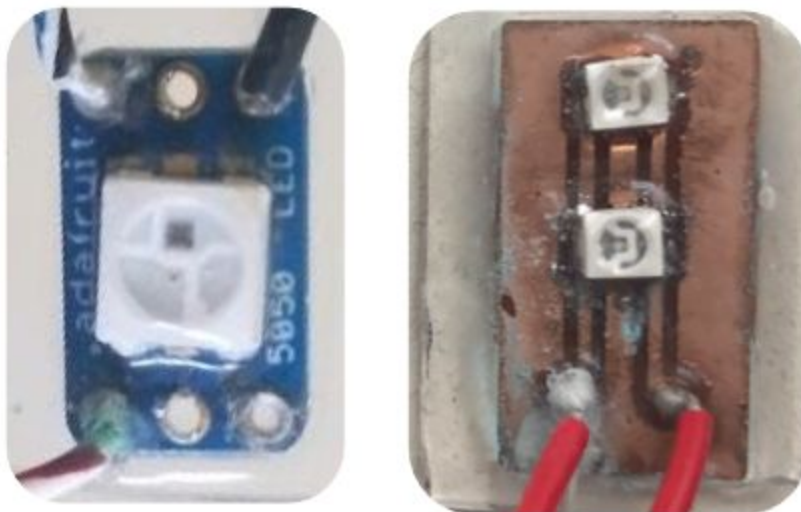
*Figure 20. Corrosion of both 405nm and 465nm LEDs was evident after three replicates of testing for a duration of 2 hours (six hours of testing altogether). This suggests that after six hours of in vivo testing, the LED would no longer be suitable in the Ai32 and KikGR33 mouse models.*

The LED prototypes has potential for other disease tracking uses other than for tuberculosis. In a present-time application, the LED prototypes can help identify immune trafficking targeted therapies in KikGR33/K18-hACE2 (a murine COVID-19 transgenic mouse model) to suppress hyperinflammation in COVID-19 for patients suffering from acute respiratory distress syndrome. Future work for further development of the LED prototypes would be coating the LEDs in veterinary grade epoxy resin due to the corrosion and poor encapsulation of the PCB by the PDMS. Additional *in vitro* and *in vivo* testing is necessary for proof of concept. We have already shown that the 405nm LEDs are functional with the KikGR33 mouse model in an *in vitro* test. *In vitro* testing with the 465nm LEDs would be necessary to show proof of concept for photoactivation of the Ai32 mouse model. Further testing will need to be done with coated LEDs to understand phototoxicity thresholds for intensity and duration. The end-goal of this project would be *in vivo* testing to test whether LEDs are suitable alternatives to fiber optics for photoconversion and photoactivation of KikGR33 and Ai32 mouse models.

## 5. Acknowledgements

## 6. References

[1]      "Global tuberculosis report 2018," World Health Organization, 11-Sep-2019. [Online]. Available: https://www.who.int/tb/publications/global_report/en/. [Accessed: 08-Oct-2019]. https://www.nationalgeographic.org/encyclopedia/bioluminescence/. [Accessed: 10-Oct-2018].

[2]      S. A. Marcus, M. Herbath, Z. Fabry, and M. Sandor, "Dynamic changes in Mycobacterium tuberculosis-induced granulomas: developing new tools," The Journal of Immunology, 01-May-2018. [Online]. Available:https://www.jimmunol.org/content/200/1_Supplement/117.19. [Accessed:

08-Oct-2019].

[3]     C. Bussi and M. G. Gutierrez, "Mycobacterium tuberculosis infection of host cells in space and time," FEMS microbiology reviews, 01-Jul-2019. [Online]. Available: https://www.ncbi.nlm.nih.gov/pmc/articles/PMC6606852/. [Accessed: 08-Oct-2019].

[4]     "STOCK Tg)CAG-KikGR)33Hadj/J Overview," 013753 - STOCK Tg(CAG-KikGR)33Hadj/J. [Online]. Available: https://www.jax.org/strain/013753. [Accessed: 08-Oct-2019].

[5]     M. Tomura, A. Hata, S. Matsuoka, F. H. W. Shand, Y. Nakanishi, R. Ikebuchi, S. Ueha, H. Tsutsui, K. Inaba, K. Matsushima, A. Miyawaki, K. Kabashima, T. Watanabe, O. Kanagawa, "Tracking and quantification of dendritic cell migration and antigen trafficking between the skin and lymph node," Scientific Reports, vol. 4, no. 6030, Aug. 2014. [Online] Available: https://www.ncbi.nlm.nih.gov/pmc/articles/PMC4129424/

[6]     M. Tomura, N. Yoshida, J. Tanaka, S. Karasawa, Y. Miwa, A. Miyawaki, O. Kanagawa, "Monitoring cellular movement in vivo with photoconvertible fluorescence protein "Kaede" transgenic mice," Proceedings of the National Academy of Sciences of the United States of America, vol. 105, no. 31, pp. 10871-10876. [Online]. Available: https://www.ncbi.nlm.nih.gov/pmc/articles/PMC2504797/

[7]     Reichert, W. (2008). Indwelling Neural Implants: Strategies for Contending With the in Vivo Environment (Frontiers in neuroengineering). CRC Press, Chapter 3.

[8]     J. Heisterkamp, R. van Hillegersberg, J.N. Ijzerman. (1999). Critical temperature and heating time for coagulation damage: implications for interstitial laser coagulation (ILC) of tumors. Lasers in Surgery and Medicine. Available at: https://www.ncbi.nlm.nih.gov/pubmed/10495303

[9]     S. Hornm "Silicone Conformal Coating vs. Parylene," Diamond-MT, Conformal Coating, August. 7, 2015. [Online]. Available: https://blog.paryleneconformalcoating.com/silicone-conformal-coating-vs-parylene. [Accessed:

December 9, 2019].

[10]    S. Ahn, J. Jeong, S. J. Kim, "Emerging Encapsulation Technologies for Long-Term Reliability of Microfabricated Implantable Devices," Micromachines (Basel), vol. 10, no. 8, pp. 508. 2019. [Online]. Available: https://www.ncbi.nlm.nih.gov/pmc/articles/PMC6723304/

[11]    Specialty Coating Systems (2007) "Parylene Properties," Specialty Coating Systems. [Online] Available: https://www.physics.rutgers.edu/~podzorov/parylene%20properties.pdf. [Accessed: December 10, 2019].

[12]    D. S. Lee, S. J. Kim, E. B. Kwon, C. W. Park, S. M. Jun, B. Choi, S. W. Kim, "Comparison of in vivo biocompatibilities between parylene-C and polydimethylsioxane for implantable microelectronic devices," Bulletin of Materials Science, vol. 36, no. 6, pp. 1127-1132. [Online]. Available: https://www.ias.ac.in/article/fulltext/boms/036/06/1127-1132

[13]    M. Tomura, T. Honda, K. Tanizaki, A. Otsuka, G. Egawa, Y. Tokura, H. Waldmann, S. Hori, J. G. Cyster, T. Watanabe, Y. Miyachi, O. Kanagawa, K. Kabashima, "Activated regulatory T cells are the major T cell type emigrating from the skin during a cutaneous immune response in mice, " The Journal of Clinical Investigation, vol. 120, no. 3, pp. 883-893. [Online]. Available: https://www.ncbi.nlm.nih.gov/pmc/articles/PMC2827959/

[14]    A. Prabhakar, D. Vujovic, L. Cui, W. Olson, W. Luo, B. Arenkiel, "Leaky expression of channelrhodopsin-2 (ChR2) in Ai32 mouse lines," PLOS One, vol. 14, no. 3. [Online]. Available: https://www.ncbi.nlm.nih.gov/pmc/articles/PMC6435231/

[15]    L. Madisen, T. Mao, H. Koch, J. Zhuo, A. Berenyi, S. Fujisawa, Y. A. Hsu, A. J. Garcia III, X. Gu, S. Zanella, J. Kidney, H. Gu, Y. Mao, B. M. Hooks, E. D. Boyden, G. Buzsaki, J. M. Ramirez, A. R. Jones, K. Svoboda, X. Han, E. E. Turner, H. Zeng, "A toolbox of Cre-dependent optogenetic transgenic mice for light-induced activation and silencing," Nature Neuroscience, vol. 15, no. 5, pp. 793-802. [Online]. Available: https://www.ncbi.nlm.nih.gov/pmc/articles/PMC3337962/

[16]    USHIO, Deep UV Lamp Spot-Cure Series - Spot UV Curing Equipment, Tokyo

Instruments, 2019. Accessed on: December. 9, 2019. [Online]. Available:
http://www.tokyoinst.co.jp/en/products/detail/UD02/index.html

[17]     Blue Sky Research, Fiber Coupled Lasers, Blue Sky Research, 2019. Accessed on:
December. 9, 2019. [Online]. Available:
https://blueskyresearch.com/products/fiber-coupled-lasers-and-systems/fiber-coupled-lasers/

[18]     Mouser Electronics. (2020). VLMU3100-GS08 Vishay Semiconductors | Mouser. [online]
Available at:
https://www.mouser.com/ProductDetail/Vishay-Semiconductors/VLMU3100-GS08?qs=sGAEpi
MZZMsl8UZd3ZuU6YZ3nvPDyevX9oPcBaE1QHc%3D [Accessed 26 Feb. 2020].

[19]     Industries, A. (2020). NeoPixel 5050 RGB LED with Integrated Driver Chip - 10 Pack.
[online] Adafruit.com. Available at: https://www.adafruit.com/product/1655 [Accessed 26 Feb.
2020].

[20]     A. I. Farrer, H. Odéen, J. D. Bever, B. Coats, D. L. Parker, A. Payne, and D. A.
Christensen, "Characterization and evaluation of tissue-mimicking gelatin phantoms for use with
MRgFUS," Journal of Therapeutic Ultrasound, vol. 3, no. 1, 2015.

[21]     "Rotary Potentiometer - Linear (10k ohm)," *Sparkfun*. [Online]. Available:
https://www.sparkfun.com/products/9288. [Accessed 29 Apr 2020].

## 7.  Supplementary Data/Figures:

*7.1.*   Wavelength and Intensity Calculations

For the LED intensity and wavelength testing, the data had to be further analyzed because
the USB 2000+ gives a light intensity measured in counts every 100ms, and for our purposes
intensity should be in units of mW/cm$^2$. Every count of photon energy is calculated with $h*c/\lambda$
where h is Planck's constant, c is the velocity of light, and $\lambda$ is the wavelength measured
(Equation 1). Since the counts are measured within 100ms, the number of counts in one second
is 10 times more than the counts in 100 ms. The USB2000+ has a light sensitive array with

2048 pixels which is 14µm x 200µm [6]. Then, the light intensity within a certain area may be calculated by the light energy divided by the pixel area (Equation 2).

$$E = counts * \frac{1s}{100ms} * \frac{h*c}{\lambda}$$   **Equation (1)**

$$light\ intensity\ per\ area = \frac{E}{Area}$$   **Equation (2)**

By using these 2 equations, the spectrophotometer intensity data could be converted into the light intensity units of mW/cm^2.

*7.2.*    405nm Voltage vs. Intensity Testing Setup

A potentiometer was placed between power and the power input of the 405 nm LED to control the intensity of the light. (Fig. 21). There are three pins on the potentiometer. The output pin of the potentiometer is the middle pin. The two outer pins are connected to either ground or power (there is no preference for which of the outer pins connect to).
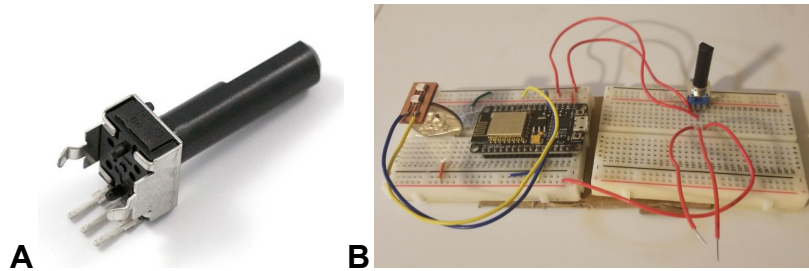


**A**          **B**

*Figure 21. A, The three pin linear rotary potentiometer features a dial that will increase or decrease resistance. The potentiometer was obtained from Sparkfun [21]. B, Testing set-up with implementation of the potentiometer for wavelength and intensity analysis with variable voltage. The two unconnected wires to the potentiometer are used to measure the voltage with a digital multimeter.*

**Appendix:**

**Product Design Specifications (PDS)**

**Function:**
The discovery of microbial opsin genes, which is a group of genes that was first studied in neurons, makes it possible to selectively control activation or silencing of neurons or other cells by light. Optogenetics is the study that combines optics with tissue genetically modified to

express light-sensitive channels in the cell membrane. Our client aims to study immune trafficking in tuberculosis and inflammation of the brain by using optogenetics [1]. Our group's product will be safe to be implanted in mice and should emit light within certain wavelength requirement. The light source can also be switched on and off easily by operator for research use. The light's intensity is able to trigger all of the light sensitive channels inside the mouse tissue.

**Client requirements:**

The goal of our client is to use optogenetic activation or blocking of neurons to alter immune cell functions in mice to understand inflammatory responses in brain and lung diseases [1]. In vivo light delivery is key to this project and our client needs a solution for 480nm and possible 405nm light that can deliver light to a larger area, which is about one square centimeter, and can be switched on and off for specific increments in the mice. The heat produced by the light should neither be harmful nor kill the cells and tissues near implantation site. The light should be delivered deep enough to stimulate the lung tissue of the mice without causing harmful phototoxicity. The light should also be reusable if it is expensive to fabricate.

**Design requirements:**

1. Physical and Operational Characteristics

a. Performance requirements:

  The device will be turned on for the complete duration of the experiment which will last for two hours. Not only does the device need to be powered for the duration of the experiment, it must continue to be functional and biocompatible under physiological conditions within the mouse's subcutaneous tissue (wet, temp: 36.9 °C, pH: 6-8) [2].

  Light must have a size of approximately one square centimeter with a broad light source range able to penetrate deep into the organs of the mice. It also needs to have a wavelength of 405nm and/or 480nm without producing UV rays that may damage the tissue.

  Light source must be able to be switched on and off for 15-30 second intervals over each 2-hour experiment. The light source must be flexible and able to be inserted subcutaneously to the mice's skull.

b. Safety:

  The heat generated by light should be minimal and not be harmful to neighboring cells and tissues. The thermal tolerance for implantable devices is approximately 1 degree celsius. During the duration of the experiment, the device should be able to diffuse the heat from the light emitting diode to prevent thermal damage. In addition, the team should make sure the UV light is not produced by the light source as the UV light would cause harm to the cells. The device should also be designed to limit phototoxicity of the living tissue. The material should also be biocompatible so that it will not cause an inflammatory response in the tissue. Electronic

components of the device will be coated in a biocompatible and implantable material (example parylene C or PDMS) to prevent voltages and currents from harming the mice.

c. Accuracy and Reliability:

The light needs to be durable and biocompatible so that it is able to withstand the environment inside the blood vessels of mice. Also, the light source developed should be broad enough to cover enough areas on the organs of the mice to make sure the light-sensitive genes can be triggered and monitored. The light emitting diodes should emit wavelengths of 405nm and 480nm.

d. Life in Service:

Ideally the electrical components of the device will be reusable while the coating biomaterial would be covering the light and could be sterilized by ethanol. The light source should also work continuously and consistently without unpredicted damage in the hardware. The heat sink would also aid performance in maintaining the energy from dissipating in the form of heat to maintain light intensity for the time during use.

e. Operating Environment:

The device will be exposed to physiological conditions in the subcutaneous tissue of the mice in the chest and cranium. The device will be exposed to the body temperature and pH of the mice which is approximately 36.9 °C and pH 6-7, respectively [2]. Since the device is in an aqueous, saline environment, there is risk of corrosion and/or electric shock. The individuals at risk are the mouse itself or the person carrying out the experiment and this risk must be mitigated.

f. Ergonomics:

The device should be readily and easily picked up using tweezers. Once the device is in the mouse, it will not be handled by a human until it needs to be removed - a microcontroller will simply need to be turned on to operate the device.

g. Aesthetics, Appearance, and Finish:

The design needs to be small, compact, and streamlined. Since the design will be used *in vivo*, wires are acceptable but not preferred. The materials used need to be durable and able to function when in the subcutaneous environment of the mice. The device needs to be biocompatible and prevent any form of liquid from seeping into the device.

2. Production Characteristics

a. Target Product Cost:

The client did not specify the budget as long as we make reasonable use of the money provided by our client. Our team will try to minimize the amount we might spend and try to make our device reusable and reliable.

3. Miscellaneous

a. Standards and Specifications:  FDA Regulation of Implantable Medical Devices
Our device to be built will be implanted subcutaneously in the mouse. According to the FDA the ambient temperature must not increase by more than 1°C or brain damage may occur [3].

b. Customer:
For a preliminary design specification in regard to customer, the device should be user-friendly (easy to handle, will not fall apart easily when mishandled, etc). This device will not be available to the commercial consumer - it will be used for research purposes at the client's research lab.

c. Patient-related concerns:
Our design will not be applied to patients directly even though the ultimate goal might be to alter immune response of humans. For our research subjects, mice, the use of light source must not be detrimental to the research projects and the device should be safe to mice when being implanted.

d. Competition:
1. Biocompatible optical fiber-based nerve cuff can be used for light delivery that wraps around the target neuron. The research mainly considers light delivery to peripheral axons [3].
2. Epidural fiber-optic implants:
Epidural fiber is used in light delivery for spinal cords. The system [4] enables sufficient light intensity and different light wavelength to be delivered.

References:

[1] Fabry, Z., Chreiber, HS., Harris, MG., Sandor, M. (2008). Sensing the  microenvironment of the central nervous system: immune cells in the central nervous system and their pharmacological manipulation. *Curr Opin Pharm.* doi: 10.1016/j.coph.2008.07.009.

[2] The Staff of the Jackson Laboratory. Biology of the Laboratory Mouse. New York: *Dover Publications INC.*, 1966.

[3] Reichert, W. (2008). Indwelling Neural Implants: Strategies for Contending With the in Vivo Environment (Frontiers in neuroengineering). CRC Press, Chapter 3.

[4] Towne, C., Montgomery, K. L., Iyer, S. M., Deisseroth, K., & Delp, S. L. (2013). Optogenetic Control of Targeted Peripheral Axons in Freely Moving Animals. *PLoS ONE,8*(8). doi:10.1371/journal.pone.0072691

[5] Bonin, R. P., Wang, F., Desrochers-Couture, M., Ga¸secka, A., Boulanger, M., Côté, D. C., & Koninck, Y. D. (2016). Epidural optogenetics for controlled analgesia. *Molecular Pain,12*, 174480691662905. doi:10.1177/1744806916629051